HHS Public Access

Author manuscript

Glia. Author manuscript; available in PMC 2021 August 10.

Published in final edited form as:

Glia. 2020 March ; 68(3): 617–630. doi:10.1002/glia.23743.

Developmental stage-specific role of Frs adapters as mediators of FGF receptor signaling in the oligodendrocyte lineage cells

Miki Furusho[1], **Akihiro Ishii**[1], **Jean M. Hebert**[2], **Rashmi Bansal**[1]

[1]Department of Neuroscience, University of Connecticut Medical School, Farmington, Connecticut

[2]Department of Neuroscience, Albert Einstein College of Medicine, Bronx, New York

Abstract

FGF signaling is important for numerous cellular processes and produces diverse cellular responses. Our recent studies using mice conditionally lacking FGF-Receptor-1 (Fgfr1*)* or Fgfr2 during different stages of myelinogenesis revealed that Fgfr signaling is first required embryonically for the specification of oligodendrocyte progenitors (OPCs) and then later postnatally for the growth of the myelin sheath during active myelination but not for OPC proliferation, differentiation, or ensheathment of axons. What intracellular signal transduction pathways are recruited immediately downstream of Fgfrs and mediate these distinct developmentally regulated stage-specific responses remain unclear. The adapter protein Fibroblast-Growth-Factor-Receptor-Substrate-2 (Frs2) is considered a key immediate downstream target of Fgfrs. Therefore, here, we investigated the in vivo role of Frs adapters in the oligodendrocyte lineage cells, using a novel genetic approach where mice were engineered to disrupt binding of Frs2 to *Fgfr1* or *Fgfr2*, thus specifically uncoupling Frs2 and Fgfr signaling. In addition, we used conditional mutants with complete ablation of *Frs2* and *Frs3*. We found that *Frs2* is required for specification of OPCs in the embryonic telencephalon downstream of Fgfr1. In contrast, Frs2 is largely dispensable for transducing Fgfr2-mediated signals for the growth of the myelin sheath during postnatal myelination, implying the potential involvement of other adapters downstream of Fgfr2 for this function. Together, our data demonstrate a developmental stage-specific function of Frs2 in the oligodendrocyte lineage cells. This contextual requirement of adapter proteins, downstream of Fgfrs, could partly explain the distinct responses elicited by the activation of Fgfrs during different stages of myelinogenesis.

Keywords

myelin; myelination; myelinogenesis; oligodendrocyte; oligodendroglia

Correspondence Rashmi Bansal, PhD, Department of Neuroscience, University of Connecticut Medical School, 263 Farmington Ave., Farmington, CT 06030. bansal@uchc.edu.

CONFLICT OF INTEREST

The authors declare no potential conflict of interest.

1 | INTRODUCTION

Oligodendrocyte development and myelination of axons is a complex multistep process regulated by numerous signals in the CNS. Fibroblast growth factors (FGFs), which bind to four FGF tyrosine kinase receptors (Fgfr), are known to regulate diverse cellular processes and play pleiotropic roles in development and disease (Beenken & Mohammadi, 2009; Ornitz & Itoh, 2015). Fgfr1 and Fgfr2 are expressed in a developmentally regulated manner in the oligodendrocyte lineage cells and in the germinal zones of the embryonic forebrain from where OPCs are generated (Bansal, Kumar, Murray, Morrison, & Pfeiffer, 1996; Bansal, Lakhina, Remedios, & Tole, 2003; Fortin, Rom, Sun, Yayon, & Bansal, 2005). Through the analysis of a series of conditional knock-out mice, where Fgfr1/2 were ablated at different stages of myelinogenesis in the CNS, our previous studies have revealed a *biphasic* requirement of these receptors: first for embryonic specification of oligodendrocyte progenitors (Furusho, Kaga, Ishii, Hébert, & Bansal, 2011) and then subsequently for the growth of the myelin sheath during active myelination but not for proliferation, differentiation, or ensheathment of axons (Furusho, Dupree, Nave, & Bansal, 2012). From the analysis of *single* knock-out mice, we found that for the “earlier function” of oligodendrocyte progenitor specification, Fgfr1 is the more significant receptor type, while for the “later function” of myelin assembly, Fgfr2 but not Fgfr1 was needed (Furusho, Ishii, & Bansal, 2017). Thus, these data together suggest that the nature of FGF signaling required for oligodendrocyte progenitor generation from the neuroepithelial precursors and that for myelin biogenesis by mature oligodendrocytes may be interpreted somewhat differently by the cells at different phases of myelinogenesis. It remains unclear how these activated receptors at the plasma membrane might transmit these context-dependent signals. It is known that many signaling proteins bind directly to the Fgfrs and initiate multiple intracellular signaling cascades (Brewer, Mazot, & Soriano, 2016; Turner & Grose, 2010). Much of the information about the identities of these signaling proteins has been obtained from in vitro assays (mostly in cell lines). It is currently unknown which of the regulatory proteins, immediately downstream of Fgfrs, are deployed in the oligodendrocyte lineage cells in vivo for transmitting signals from Fgfrs during different stages of oligodendrocyte development and myelin assembly. The adapter protein Fibroblast Growth Factor Receptor Substrate 2 (Frs2) is known to be a key immediate target recruited by both Fgfr1 and Fgfr2 that initiates downstream signaling cascades (Brewer et al., 2016; Gotoh, 2008; Mason, 2007; Turner & Grose, 2010), notably the Ras/Raf/Mek/ERK pathway. Several studies have shown that this pathway plays a critical role in the regulation of myelin growth and maintenance (Furusho et al., 2017; Fyffe-Maricich, Schott, Karl, Krasno, & Miller, 2013; Ishii, Furusho, & Bansal, 2013; Ishii, Furusho, Dupree, & Bansal, 2014; Ishii, Furusho, Dupree, & Bansal, 2016; Ishii, Furusho, Macklin, & Bansal, 2019; Jeffries et al., 2016). Furthermore, we have shown that Frs2, like Fgfr2, is expressed in mature oligodendrocytes, is enriched in the cytoplasmic noncompact myelin compartment, co-partitions into “lipid raft” microdomains, and, at least in vitro, can be phosphorylated by Fgfr activation with concomitant ERK1/2 and Akt phosphorylation (Bryant, Marta, Kim, & Bansal, 2009). Although Fgfr1-Frs2 and Fgfr2-Frs2 interactions have been shown to play important roles in bone and kidney development (Eswarakumar et al., 2006; Sims-Lucas et al., 2011), their

in vivo role in neural development is beginning to emerge very recently (Brewer, Molotkov, Mazot, Hoch, & Soriano, 2015; Nandi et al., 2017).

In addition to mediating signals from Fgfrs, Frs2 is also known to transmit signals from a limited number of other receptor tyrosine kinases, including Trk receptors (Gotoh, 2008), providing a selective means of integrating and amplifying signals from a subset of growth factors. Given the importance of BDNF/TrkB and NT3/TrkC signaling in myelinogenesis (Du, Lercher, Zhou, & Dreyfus, 2006; Kahn et al., 1999; Xiao et al., 2010), it is possible that Frs2 may have an even more central role in myelinogenesis than simply transmitting Fgfr signals. Therefore, we hypothesize that Frs2 serves as a key "intracellular control center," linking a set of promyelinating receptor tyrosine kinases, primarily Fgfrs and Trks, to major promyelinating intracellular signaling pathways, primarily Ras/Raf/Mek/ERKs and PI3K/Akt/mTOR, in the oligodendrocyte lineage cells.

To test this hypothesis, we generated mice where Frs2/3 binding to Fgfrs is disrupted by mutating *Fgfr1* or *Fgfr2* at its Frs2/3 binding sites in a cell-specific manner. We also analyzed mice where Frs2/3 were completely ablated conditionally. We found that as hypothesized, during embryonic development, Frs2 functions as the sole mediator of Fgfr1 signaling for the specification of oligodendrocyte progenitors from the neuroepithelial cells. However, contrary to our hypothesis, during the active period of myelination, Frs2/3 by themselves are not sufficient to transduce Fgfr2-mediated signals for promoting myelin gene expression and thus myelin growth by mature oligodendrocytes. These studies reveal that Frs adapters show developmental stage-specific selectivity in their ability to mediate Fgfr signaling in the oligodendrocyte lineage.

2 | MATERIAL AND METHODS

2.1 | Generation of Frs binding site mutants of FGF receptors and Frs2/3 conditional knockout mice

We generate *Frs2-uncoupled Fgfr1/2* double-mutant mice by mating $Fgfr1^{flox/flox};Fgfr2^{\Delta Frs/+}$ (obtained from Dr. V. P. Eswarakumar, Yale University) with $Cnp^{cre/+};Fgfr1^{flox/flox};Fgfr2^{flox/flox}$ mice to produce progeny in which one allele of Fgfr2 was ablated and the other allele was mutated at the Frs2/3-binding site ($CNP^{Cre/+};Fgfr1^{flox/flox},Fgfr2^{flox/\Delta Frs2}$) leading to the disruption of Frs2/3 binding to Fgfr2 in CNP-expressing oligodendrocyte-lineage cells (2′,3′-cyclic nucleotide 3′-phosphohydrolase; Lappe-Siefke et al., 2003; Gravel et al., 1998; Tognatta et al., 2017). Fgfr1 is also ablated in these cells. These mice are referred to as $Fgfr1^{-/-};Fgfr2^{\Delta Frs/-}$. Littermates of these mutants lacking Cre are referred to as "controls". We also generated conditional double knockout mice with complete disruption of Frs2 by appropriate mating of $Frs2^{flox/flox};Frs3^{+/-}$ to produce progeny with complete disruption of Frs2 in CNP-expressing oligodendrocyte-lineage cells in an Frs3-null background ($Cnp^{cre/+};Frs2^{flox/flox};Frs3^{-/-}$) which are referred to as *Frs2/3 dKO*. This mating also generated single knockout mice of *Frs2* (referred as *Frs2 cKO*) and *Frs3* (referred as $Frs3^{-/-}$). Littermates of these mutants lacking Cre are referred to as "controls". The genetic backgrounds of $Frs2^{flox/flox};Frs3^{-/-}$ lines is C57BL/6 × 129/Svj x Swiss Webster and that of $Fgfr1^{flox/flox};Fgfr2^{\Delta Frs/flox}$ lines is C57BL/6 x CD1 × 129/Svj. Also used in this study are *Fgfr1/2 dKO* mice

(*Cnp*$^{cre/+}$;*Fgfr1*$^{flox/flox}$;*Fgfr2*$^{flox/flox}$) mice, referred to as *Fgfr1*$^{-/-}$;*Fgfr2*$^{-/-}$, which have been described previously (Furusho et al., 2012).

Also used in this study are embryos at E12.5 which have one allele of Fgfr1 mutated at the Frs2-binding site and the other allele floxed, driven by telencephalon-specific Foxg1Cre (*Fgfr1*$^{\Delta Frs/flox}$;*Fgfr2*$^{flox/+}$; *Foxg1*$^{Cre/+}$). These mice also have *Fgfr2* floxed in one allele and are referred to as *Fgfr1*$^{\Delta Frs/-}$;*Fgfr2*$^{+/-}$. Littermates of the genotype *Fgfr1*$^{+/-}$; *Fgfr2*$^{+/-}$ serves as "controls" for these mutants. E12.5 embryos from mice with complete conditional ablation of *Frs2* alone (*Foxg1Cre; Frs2*$^{flox/flox}$) or Frs2 in an Frs3-null background (*Foxg1Cre;Frs2*$^{flox/flox}$; *Frs3*$^{-/-}$) as well as Frs3-null (*Frs3*$^{-/-}$) mice were also collected. These mutants are referred to as *Frs2 cKO*, *Frs2/3 dKO* and *Frs3*$^{-/-}$ respectively. Littermates of these mutants without Cre were used as "controls". The specificity of *Frs2/3* loss in these mutant mice at E12.5 has been demonstrated previously (Nandi et al., 2017, Figure 1a,b).

2.2 | In situ hybridization

As described previously (Furusho et al., 2012; Ishii, Fyffe-Maricich, Furusho, Miller, & Bansal, 2012; Kaga et al., 2006), postnatal day 15 (P15) and 30 (P30) old mice of both sexes perfused with phosphate buffered saline (PBS) or 4% paraformaldehyde/PBS were subjected to post-fixation overnight in 4% paraformaldehyde/PBS, and then another overnight in 20% sucrose/PBS. Embryonic day (E)12.5 brains were fixed by immersion in 4% paraformaldehyde in PBS and cryoprotected sequentially in 10% sucrose followed by 30% sucrose, each carried out overnight at 4°C and embedded in OCT compound (Tissue-Teck) as described previously (Furusho et al., 2011). In situ hybridization for myelin basic protein (MBP) and proteolipid protein (PLP) was performed on transverse cryostat sections (15 um) of cervical spinal cord and for platelet derived growth factor receptor alfa (Pdgfra) on coronal cryostat sections of forebrains (30 um) as described (Furusho et al., 2011; Furusho et al., 2012; Ishii et al., 2012). Specific riboprobes for MBP mRNA (Dr. M. Qiu, Univ. of Louisville, Kentucky), PLP mRNA (Dr. W.B. Macklin, Univ. of Colorado Sch. of Med., Aurora, CO) or Pdgfra mRNA (Dr. W. D. Richardson, University Collage, London) were used. Briefly, after incubation in 1 ug/ml proteinase K at 37°C for 15–30 min, sections were hybridized overnight at 65°C with digoxigenin-labeled antisense cRNA probe, and washed in 50% formamide, 2 × SSC, and 1%SDS at 65°C for 2–3 hr, followed by rinses in 2 × SSC and 0.2 × SSC at room temperature, and 0.1 × SSC at 60°C. After blocking in 1% Tween20 and 1% normal goat serum (1 hr), sections were incubated (overnight) in alkaline phosphatase-conjugated anti-digoxigenin antibody (1:2000; Roche Diagnostics, Penzberg, Germany). Color was developed with 4-nitroblue tetrazolium chloride and 5-bromo-4-chloro-3-indolylphosphate.

ISH analysis of control and littermate mutant mice from a given line of mice was always done in an identical manner, where the sections from the control and mutant were cut at the same plane and placed on the same slide so that the in situ hybridization could be performed identically and comparisons of signal intensity could be made reliably between the mutant and controls. Quantification of the total numbers of Pdgfra mRNA positive cells in the whole caudal forebrains, obtained from E12.5 embryos from control and mutant mice

was done from three matched sections each and the data presented as percentage of controls. Analysis of samples was done blinded to the genotypes of the mice.

2.3 | Immunohistochemistry

Transverse sections (15 um) of cervical spinal cord from P15 or P30 old mice of both sexes were prepared as above. For MBP (1:3000; Dr. E. Barbarese, UCONN) immunolabeling, sections were delipidated with 100% ethanol for 10 min, washed with PBS (3 times, 10 min), blocked (1 h) in PBS, 10% normal goat serum (NGS, Invitrogen, CA), 5% BSA, and 0.1% fish gelatin. Prior to immunolabeling for p-ERK1/2 (1:400; Cell Signaling, MA) and p-Akt (Thr308; 1:100; Cell Signaling), spinal cord sections were subjected to antigen retrieval by 5 min of incubation at 95°C in citrate buffer, pH 6.0, washed with PBS (3 times, 10 min), blocked (1 h) in PBS, 10% NGS, 0.03% TritonX100. For p-mTOR (Ser2448, 1:100; Cell Signaling) and p-S6RP (Ser235/236; 1:100; Cell Signaling) immunolabeling, sections were incubated in TBSS, 5% methanol/1% H_2O_2 for 10 min, washed with TBSS (3 times, 10 min), 10% Triton X-100 for 30 min, and blocked (1 h) in TBSS, 10% NGS and then TBSS, 0.3% BSA, 0.02% TritonX-100. Specimen were incubated with primary antibody in blocking buffer at 4°C for 24–72 hr. Phosphate-buffered or Tris-buffered saline containing 100 uM sodium fluoride, 100uM o-vanadate were used for dilutions of antibodies and washes. After washing the primary antibody, the specimen were incubated in appropriate secondary antibodies conjugated to biotin (1:200; Vector Lab., CA), or Alexa 488 (1:500; Molecular Probes, CA) and nuclei were counterstained with Hoechst blue dye 33,342 (1 mg/mL; Sigma, MO). The Avidin/Biotinylated Enzyme Complex (ABC) system (Vector Lab., CA) was used to detect biotinylated secondary antibodies, and the color was developed by incubation in DAB (3,3′-diaminobenzidine, Sigma, MO). Negative controls were treated identically except for the exclusion of primary antibodies. Quantification of the MBP immunolabeled area of lateral-ventral white matter was done using the area measurement function in Photoshop. Analysis of samples was done blinded to the genotypes of the mice.

2.4 | Quantitative real-time PCR (qRT-PCR)

Total RNA from spinal cords of P15 or P30 old mice of both sexes was extracted using the TRIzol reagent (Invitrogen, Carlsbad, CA).A 1 ug total RNA was reverse-transcribed to cDNA using the iScript™ Synthesis Kit (BioRad, Hercules, CA) according to the manufacturer's instructions. qRT-PCR was performed using a CFX Connect™ Real-Time PCR Detection System (Bio-Rad, Hercules, CA) and iQ™ SYBR Green Supermix (BioRad, Hercules, CA) according to the manufacturer's instructions. qRT-PCR conditions were as follows: denaturation at 95°C, 30 s; primer annealing at 55.5°C, 30 s; and elongation at 72°C, 40 s. Quantification of PCR products was performed using the 2-ΔΔCt method. Quantities of mRNA were normalized to the housekeeping gene *GAPDH*. The following primers were used: PLP forward primer, 5′-GTATAGGCAGTCTCTGCGCTGAT-3′; PLP reverse primer, 5′-AAG TGGCAGCAATCATGAAGG-3′; MBP forward primer, 5′-TACCTGG CCACAGCAAGTAC-3′; MBP reverse primer, 5′-GTCACAATGTTCTTGAAG-3′; Glyceraldehyde-3-phosphate dehydrogenase (*GAPDH*) forward primer, 5′-TGTGTCCGTCGTGGATCTG-3′; *GAPDH* reverse primer, 5′-CATGTAGGCCATGAGGTCCACCAC-3′.

2.5 | Electron microscopy (EM)

Transgenic and littermate control mice of both sexes were perfused with 4% paraformaldehyde, 2% glutaraldehyde in 0.1 M cacodylate buffer, pH 7.4 (Electron Microscopy Sciences, Hatfield, PA). Cervical spinal cords of mice were post-fixed in 1% OsO4. Samples were dehydrated through graded ethanol, stained en bloc with uranyl acetate, and embedded in Poly/Bed812 resin (Polysciences Inc., Warrington, PA). Semithin (1 um) sections were stained with toluidine blue. Ultrathin (0.1 um) sections from matching areas of experimental and control tissue blocks were cut and visualized using an electron microscope (JEOL1200CX) at 80 kV. Digitized images (magnification 3,000X) were used to determine the g-ratios of randomly selected myelinated axons. Approximately 400 axons were measured per genotype from matched regions of the ventral cervical spinal cord. Statistical analysis was performed on average g-ratios using ANOVA. For comparison of control and mutant mice note that higher g-ratios indicates thinner myelin sheath.

2.6 | Immunoblotting

Immunoblotting was performed as described previously (Fortin et al., 2005). Briefly, equal amounts of total proteins from lysates of white matter from spinal cords of mice of both sexes were loaded onto SDS-PAGE, transferred to PVDF membranes, and immune-labelled for MBP (1:10,000; gift from E. Barbarese, University of Connecticut Medical School, Farmington, CT), phospho-Akt^{T308} (1:1000; Cell Signaling Technology), phospho-mTOR^{S2448} (1:1000; Cell Signaling, Danvers, MA), and GAPDH (1:60,000; Biodesign International, Saco, ME) as a loading control. Quantification of the bands was done by Image-J software. Statistical analysis used to evaluate immunoblots was done by one way ANOVA test.

3 | RESULTS

3.1 | Complete ablation of Frs2 or genetically uncoupling Frs2 and Fgfr1 signaling in the embryonic forebrain cells leads to severe deficits in the specification of OPCs at E12.5

We have shown previously that in the embryonic forebrain, Fgfr1–3 are expressed in the ventricular zone (Bansal et al., 2003). Conditional ablation of Fgfr1/2 using the telencephalon-specific Cre line (*Foxg1Cre)* inhibited OPC generation, demonstrating a critical requirement of FGF signaling for OPC specification from the ventral forebrain at E12.5 (Furusho et al., 2011). Here, we asked whether Frs2 and/or Frs3 adapter proteins, known to be key downstream mediators of FGF receptor signaling, play a role in this function.

We obtained different lines of mutant mice, as described in Methods and briefly outlined schematically in Figure 1a. In order to determine the overall role of Frs2 and Frs3, individually or in combination, in OPC generation, we first analyzed E12.5 embryos from control and mutants with complete ablation of *Frs2* alone (*Frs2 cKO)* or with Frs3-null (*Frs2/3 dKO)* in the forebrain and Frs3-null (Frs3$^{-/-}$), by in situ hybridization for the expression of the OPC marker Pdgfra mRNA (Figure 1b,c). We found that compared to control, there was a statistically significant reduction in the numbers of Pdgfra mRNA+ cells

in the *Frs2 cKO* and *Frs2/3 dKO* but not in the *Frs3*$^{-/-}$ embryos, suggesting a requirement of Frs2 adapter proteins for OPC specification.

Since Frs2/3 are capable of functioning downstream of few other tyrosine kinase receptors besides FGF receptors, we next asked if the observed inhibition of OPC specification by Frs2 loss was specifically due to the disruption in Fgfr-mediated signaling or was a more global effect. We therefore examined OPC specification in mutant embryos that were genetically engineered to disrupt binding of Frs2 to Fgfr1, thus specifically uncoupling Frs2 and Fgfr1 signaling while leaving Frs2 signaling via other potential receptors intact. This ablation was targeted to the embryonic forebrain precursor cells by the Foxg1Cre-mediated excision of the second floxed allele of *Fgfr1*. Analysis of E12.5 forebrains from these embryos (*Fgfr1*$^{\Delta Frs/-}$*;Fgfr2*$^{+/-}$*)* and their corresponding "controls" (*Fgfr1*$^{+/-}$*;Fgfr2*$^{+/-}$*)* for the expression of Pdgfra mRNA showed that there was an almost complete loss of Pdgfra+ OPCs in the *Fgfr1*$^{\Delta Frs/-}$*; Fgfr2*$^{+/-}$ embryos (Figure 1d,e), as was observed in the E12.5 *Fgfr1*$^{-/-}$*; Fgfr2*$^{+/-}$ embryos in our previous study (Furusho et al., 2011, Figure 5a).

We conclude that the Frs2 adapter protein is required for OPC specification from the ventral ventricular neuroepithelial cells of the embryonic forebrain and that Frs2 is a key target immediately downstream of Fgfr1 mediating this function.

3.2 | Genetically uncoupling Frs2/3 and Fgfr2 signaling in oligodendrocytes of postnatal mice fails to recapitulate the severe deficits in myelin gene expression observed in mice lacking Fgfr2

We have shown previously that conditional ablation of *Fgfr2* in oligodendrocytes leads to a downregulation of myelin gene expression and attenuation of myelin growth during the active phase of myelination, demonstrating an important role of Fgfr2 signaling in the regulation of myelin assembly in the CNS (Furusho et al., 2012; Furusho et al., 2017). However, it is not known which signaling proteins, immediately downstream, are used in oligodendrocytes in vivo to initiate signaling pathways from Fgfr2 that regulate myelin gene expression and myelin growth. Since Frs2/3 adapter proteins are known to be major immediate targets recruited by Fgfrs that initiate distinct downstream signaling cascades, we asked whether Fgfr2 uses Frs2/3 adapters in oligodendrocytes to regulate myelin gene expression (Figure 2). We obtained genetically engineered mice in which Fgfr2 was rendered incapable of binding to Frs2/3, due to a point mutation in the binding site of Fgfr2. In these mice, specific downstream signaling pathways emerging from Frs2 are uncoupled from Fgfr2 while leaving all others intact (Eswarakumar et al., 2006). To achieve oligodendrocyte-specific uncoupling of Fgfr2 signaling from Frs, we bred a line of mice in which one allele of *Fgfr2* was floxed and another was mutated at the Frs2 binding site with the oligodendrocyte-specific CNP^{Cre}-driver line. We also conditionally ablated *Fgfr1* in the *Fgfr2* mutant oligodendrocytes to ensure elimination of any potential compensation by Fgfr1, even though our previous studies had indicated that Fgfr2, not Fgfr1, is the primary transmitter of FGF signals during active myelination (Furusho et al., 2017). These mice, referred to as *Fgfr1*$^{-/-}$*;Fgfr2*$^{\Delta Frs/-}$, were compared to those completely lacking *Fgfr1* and *Fgfr2* in oligodendrocytes (referred to as *Fgfr1*$^{-/-}$*;Fgfr2*$^{-/-}$ mice).

We examined MBP and PLP mRNA expression in these mice at P15 and P30 by in situ hybridization using matched sections of cervical spinal cord from mutants and littermate controls. As expected, we found a clear reduction in their signal intensity in the *Fgfr1*$^{-/-}$;*Fgfr2*$^{-/-}$ compared to control mice at both time points (Figure 2a,b). The *Fgfr1*$^{-/-}$;*Fgfr2*$^{\Delta Frs/-}$ mice showed a slight reduction in the MBP and PLP mRNA signal, especially at P15; however, it was not nearly as much as that observed in the *Fgfr1*$^{-/-}$;*Fgfr2*$^{-/-}$ mice. Quantification of mRNA levels by qRT-PCR in P15 and P30 spinal cords confirmed these observations and showed a statistically significant reduction in the expression of MBP and PLP mRNA levels in the *Fgfr1*$^{-/-}$;*Fgfr2*$^{-/-}$ but only a trend towards a reduction in the *Fgfr1*$^{-/-}$;*Fgfr2*$^{\Delta Frs/-}$ mice compared to controls (Figure 2c; dotted line shows control values set at 1).

We conclude that the decrease of myelin gene expression normally observed following complete ablation of *Fgfr2* in oligodendrocytes can not be totally recapitulated by uncoupling Frs2/3 signaling from Fgfr2, suggesting that targets other than (or in addition to) Frs2/3 are used by Fgfr2 for the regulation of myelin gene expression during the period of active myelin growth.

3.3 | Complete ablation of *Frs2/3* in oligodendrocytes of the postnatal spinal cord also fails to recapitulate the deficits in myelin gene expression observed in the conditional *Fgfr2* knock-out mice

Since, in addition to Fgfrs, Frs2 is also known to transmit signals from a limited number of other RTKs, including Trk receptors, which play important roles in myelinogenesis, we predicted that Frs2 may have a more global role in myelinogenesis. Therefore, we examined the consequences of complete conditional ablation of *Frs2/3* in OL-lineage cells. Although Frs2 is believed to be the primary relevant isoform, to ensure elimination of potential compensation by Frs3, we used a line of *Frs2-floxed* mice that were also null for *Frs3* (*CnpCre;Frs2*$^{flox/flox}$*; Frs3*$^{-/-}$, referred to as *Frs2/3 cKO*).

We examined MBP and PLP mRNA expression in these mice by in situ hybridization on cervical spinal cord sections at P15 and P30. As expected, we found that compared to control mice, there was a clear reduction in their signal intensity in the *Fgfr2* cKO at both the time points (Figure 3a,b). The *Frs2/3 cKO* mice showed a slight reduction in the MBP mRNA signal, especially at P15, however it was minor compared to that observed in the *Fgfr2 cKO* mice. Quantification of mRNA levels by qRT-PCR in P15 spinal cords confirmed these observations and showed that compared to controls, there was a statistically significant reduction in the expression of MBP and PLP mRNA levels in the *Fgfr2 cKO* but not in the *Frs2/3 cKO* mice (Figure 3c).

We conclude that the decrease of myelin gene expression observed following ablation of the complete Fgfr2 receptor in oligodendrocytes can not be totally recapitulated by complete ablation of Frs2/3 signaling. This indicates that during the period of active myelination, Frs2/3 adaptors have a dispensable role in mature oligodendrocytes, not only as key mediators of signals from Fgfr2 but also from other receptor tyrosine kinases that are known to bind to Frs2/3 and regulate myelin growth.

3.4 | Genetically uncoupling Frs2/3 and Fgfr2 signaling in oligodendrocytes fails to show a downregulation of myelin basic protein expression or a reduction in white matter area as observed in mice lacking *Fgfr2*

We have previously shown that conditional ablation of *Fgfr1/2* or *Fgfr2* alone in oligodendrocytes leads to a downregulation of myelin protein expression. Furthermore, attenuation of myelin growth and the reduction in myelin thickness observed in the *Fgfr1/2 dKO* and *Fgfr2 cKO* mice led to a significant reduction in the overall size of the white matter in the spinal cords of these mice relative to littermate controls (Furusho et al., 2012; Furusho et al., 2017). We therefore asked whether uncoupling Frs2 signaling from Fgfr2 would result in similar deficits. We immunolabeled spinal cord sections from P30 control, $Fgfr1^{-/-};Fgfr2^{-/-}$, $Fgfr1^{-/-};Fgfr2^{+/-}$, and $Fgfr1^{-/-};Fgfr2^{\Delta Frs/-}$ mice for MBP expression (Figure 4a). We found that as expected, the intensity of MBP signal and the size of the white matter area were reduced in $Fgfr1^{-/-};Fgfr2^{-/-}$ mice compared to control or $Fgfr1^{-/-};Fgfr2^{+/-}$ mice (which also serves as control). However, a similar reduction was not observed in the $Fgfr1^{-/-};Fgfr2^{\Delta Frs/-}$ mice. Quantification of the total area of the MBP+ lateral-ventral white matter (LVWM) confirmed these observations and showed a statistically significant decrease in the size of the white matter in the $Fgfr1^{-/-};Fgfr2^{-/-}$ compared to control and $Fgfr1^{-/-};Fgfr2^{+/-}$, but no such reduction was observed in the $Fgfr1^{-/-};Fgfr2^{\Delta Frs/-}$ mice (Figure 4b). We also quantified the MBP protein expression by immune blotting and found that there was no significant difference between $Fgfr1^{-/-};Fgfr2^{\Delta Frs/-}$ or *Frs2/3 cKO* mice compared to their respective controls (Figure 4c).

We conclude that as seen for MBP mRNA expression, the deficits in MBP protein expression or the size of the white matter, observed in mice lacking Fgfr2 could not be recapitulated by genetically uncoupling Fgfr2 signaling from Frs2.

3.5 | Complete ablation of Frs2/3 in oligodendrocytes did not lead to a significant reduction in myelin thickness in the spinal cords of adult mice

We have previously shown that conditional ablation of *Fgfr1/2* or *Fgfr2* alone in oligodendrocytes leads to an attenuation of myelin growth and the reduction in myelin thickness during the active phase of developmental myelination (Furusho et al., 2012; Furusho et al., 2017). In order to determine if there were similar deficits in myelin growth in the *Frs2/3 cKO* mice, we examined the ultrastructure of myelin in the spinal cords of these mice by EM analysis at 5 months of age. We found that the thickness of myelin in the *Frs2/3 cKO* mice appeared similar to their littermate controls (Figure 5a). We further quantified the myelin thickness by g-ratio measurements for individual myelinated axons relative to their respective diameters (Figure 5b). Although, there appeared to be a slight trend toward a decrease of myelin thickness, indicated by minor increase in g-ratios in the *Frs2/3 cKO* mice (average g-ratios 0.762 ± 0.004) compared with the control mice (average g-ratios 0.736 ± 0.004, $p = 9.35 \times 10^{-7}$), it was clearly not as significant as that observed previously in the *Fgfr2 cKO* (Furusho et al., 2017, Figure 3).

We conclude that the decrease of myelin thickness that we had previously observed following conditional ablation of Fgfr1/2 or Fgfr2 receptor in oligodendrocytes (Furusho

et al., 2012; Furusho et al., 2017) could not be totally recapitulated by complete ablation of Frs2/3 signaling.

3.6 | Expression of p-ERK1/2 is partly reduced but p-Akt, p-mTOR, and p-S6RP remain unchanged in oligodendrocytes of mice that have disruption of Frs2/3 binding to Fgfr2 or are completely lacking Frs2/3

We have recently shown the functional requirement of ERK1/2 as downstream mediators of Fgfr2 signaling in the regulation of myelin gene expression and myelin growth during active myelination (Furusho et al., 2017; Ishii et al., 2012). Since a key role of Frs2/3 adaptor proteins has been proposed as activator of ERK1/2 signaling downstream of Fgfrs (Turner and Grose 2010; Brewer et al., 2016), we asked whether disruption of Fgfr2-Frs2/3 interactions in oligodendrocytes would have an effect on the expression of p-ERK1/2 in the mutant mice. To address this question we immunolabeled spinal cord sections from P15 control, $Fgfr1^{-/-};Fgfr2^{+/-}$, and $Fgfr1^{-/-};Fgfr2^{\Delta Frs/-}$ mice and examined p-ERK1/2 expression in the white matter (Figure 6a). We have previously shown that p-ERK1/2 is expressed in mature oligodendrocytes, as well as in the cytoplasmic paranodal regions of myelin. Specifically, immunolabeling for phospho-ERK1/2 on teased fibers from spinal cord white matter, where paranodes and internodes can be easily distinguished, showed a strong signal of phospho-ERK1/2 in the cytoplasmic paranodal regions of myelinated fibers but not in the compacted internodal regions (Ishii et al., 2014, Figure 1C). This ERK1/2 staining seen at paranodes of teased fibers appear as a “ring-like” structures in transverse sections of the spinal cord white matter, suggestive of its localization at the paranodes and not internodes. Consistent with these studies, here also transverse sections of the spinal cord white matter from control (and $Fgfr1^{-/-};Fgfr2^{+/-}$) mice showed strong “ring-like” staining of p-ERK1/2, as well as a cellular oligodendrocyte-like staining. This “ring-like” staining of p-ERK1/2 appeared dramatically reduced in the $Fgfr1^{-/-};Fgfr2^{\Delta Frs/-}$ mice compared to controls. It is to be noted that although the p-ERK1/2 signal in the oligodendrocyte-like cell bodies appeared somewhat reduced compared to control, it was not completely lost, as was previously observed in the complete conditional *Fgfr2 cKO* or the *Fgfr1/2 dKO* mice (Furusho et al., 2017, Figure 9). Similarly, in the *Frs2/3 cKO* mice (Figure 6b), although the oligodendrocyte-like cellular signal appeared to be only partly reduced compared to control and $Frs3^{-/-}$ mice, the abundance of p-ERK1/2 positive “ring-like” structures was clearly reduced in these mice. This decrease was confirmed by quantification of the numbers of these “ring-like” structures in matched regions of the lateral-ventral spinal cord white matter of control and mutant mice (numbers of “rings” counted in the white matter of control = 440.09 ± 32.9, and in the *Frs2/3 cKO* = 78.82 ± 9.2mm^2).

We have recently shown that Fgfr2-mediated regulation of myelin gene expression and myelin growth via ERK1/2 involves signaling through mTORC1 in an Akt-independent manner (Furusho et al., 2017; Ishii et al., 2019). Specifically, we had found a reduction in the expression of p-mTOR^{S2448} and p-S6RP$^{S235/236}$ but not pAkt^{308} in the *Fgfr2 cKO* and *Fgfr1/2 dKO* mice (Furusho et al., 2017, Figure 9). We therefore asked whether the expression of p-mTOR^{S2448} and p-S6RP$^{S235/236}$ was reduced similarly in $Fgfr1^{-/-};Fgfr2^{\Delta Frs/-}$ mice (Figure 6a). Immunolabeling of spinal cord section from control, $Fgfr1^{-/-};Fgfr2^{+/-}$, and $Fgfr1^{-/-};Fgfr2^{\Delta Frs/-}$ mice showed that there was no

downregulation of the cellular signal intensity of p-mTOR^{S2448} or p-S6RP$^{S235/236}$ in the *Fgfr1*$^{-/-}$*; Fgfr2*$^{\Delta Frs/-}$ mice compared to control (and *Fgfr1*$^{-/-}$*;Fgfr2*$^{+/-}$). p-Akt^{308} expression levels remained unchanged, as expected. Similarly, cellular signal for p-mTOR^{S2448} and p-Akt^{308} in the *Frs2/3 cKO* also remained comparable to control and Frs3−/− mice (Figure 6b). Quantification of pAkt^{308} and p-mTOR^{S2448} expression by immuneblotting further confirmed that their expression levels remained unchanged in *Fgfr1 −/−;Fgfr2ΔFrs/−* and *Frs2/3 cKO* mice compared to their respective controls (Figure 6c).

We conclude that disruption of Frs2/3 adapter proteins binding to Fgfr2 or its complete loss from oligodendrocytes during active myelination has no significant effect on p-ERK1/2, p-mTOR^{S2448}, p-S6RP$^{S235/236}$ or p-Akt^{308} expression in oligodendrocytes.

4 | DISCUSSION

Using a novel genetic approach, here, we investigated the functional significance of Frs2 signaling in oligodendrocyte lineage cells. Frs2 is widely considered the primary adapter protein recruited immediately downstream of Fgfr1 and Fgfr2. Our present study supports the idea that Frs2 is an important signaling protein used by Fgfr1 in vivo to induce the specification of OPCs early during embryonic development. However, during the postnatal period of active myelin growth, Frs2/3 engagement by Fgfr2 in mature oligodendrocytes is not sufficient by itself to upregulate myelin gene expression and thus myelin assembly. Collectively, our data indicate a developmental stage-specific role of Frs2 in the oligodendrocyte lineage cells, where it is sufficient for transmitting information from Fgfr during the *early stage* but not the *late stage* of myelinogenesis.

An important function of FGF receptor signaling in the induction of oligodendrocyte progenitors during embryonic development became apparent when we observed an almost complete absence of Pdgfra- and Olig2-expressing OPCs in the ventral forebrains of E12.5 embryos lacking Fgfr1/2 (Furusho et al., 2011). In the present study, simply uncoupling Fgfr1 and Frs2 signaling completely recapitulated this phenotype, strongly suggesting that Frs2 adapter, recruited by Fgfr1, is sufficient to transmit all needed signals for OPC specification. Other recent studies using a similar genetic approach (Brewer et al., 2015; Nandi et al., 2017) that investigated the role of Frs adapters in CNS development found that while some of the functions of Fgfr1 were recapitulated in the *Fgfr1-Frs2* uncoupled mutants, others did not fully mimic the phenotype of mice lacking *Fgfr1* completely. Thus, while our study demonstrates that Frs2 is the sole mediator of Fgfr1 signaling for OPC specification, it is not the case for all Fgfr1-mediated functions during neural development, suggesting that Frs2 requirement by Fgfr1 is highly context-dependent.

During the postnatal period of active myelination, we have recently shown a key role of Fgfr2, not Fgfr1, in differentiated oligodendrocytes, where it transmits signals specifically for the upregulation of myelin gene expression and myelin growth (Furusho et al., 2017). Given the importance of Frs2 during early development (above) and our in vitro findings showing that stimulation of purified oligodendrocytes by FGF2 leads to a robust phosphorylation of Frs2 and ERK1/2 (Bryant et al., 2009), we had hypothesized that Frs2 plays a major role in transmitting Fgfr2 signals in differentiated oligodendrocytes

in vivo for the regulation of myelin gene expression and myelin growth. Surprisingly, despite the predicted important role of Frs2 in Fgfr-signaling, we observed only a minor deficit in myelin gene expression when we genetically disrupted Frs2/3 binding to Fgfr2 in oligodendrocytes of transgenic mice. Thus, contrary to our hypothesis, the phenotype of the Frs2-uncoupled-Fgfr2 did not fully recapitulate the phenotype of the *Fgfr2-KO* mice, indicating that in contrast to early development, Frs adapters are insufficient by themselves to mediate the late-stage function of FGF signaling within the oligodendrocyte lineage cells. It is known that in addition to Frs2, activated Fgfrs recruit several other signaling proteins in vitro (Eswarakumar et al., 2006), including Crk, Crkl, and Grb14 adapter proteins and Plc-gamma, which directly bind to the Fgfrs and lead to the activation of downstream signaling pathways (Brewer et al., 2016). Therefore, the lack of a more significant response in mature oligodendrocytes, in contrast to embryonic neuroepithelial cells, can potentially be due to one of the following reasons. First, Fgfrs may use different adapters during different developmental stages of oligodendrocytes to activate different downstream signaling pathways, leading to differential responses. Second, other immediate targets, such as Plc-gamma, may be compensating for the loss of Fgfr2-Frs2 signaling in oligodendrocytes. Third, cumulative activities of multiple signaling proteins/adapters, in addition to Frs2, recruited by Fgfr2 may be required within mature oligodendrocytes for the upregulation of myelin gene expression and myelin growth. Consistent with this notion, a recent study using a similar in vivo approach showed that when *Fgfr1* was mutated singly or in combinations at different sites in vivo, rendering it unable to bind to one or more of the immediate target signaling proteins, no single mutation was able to fully recapitulate the phenotype of complete *Fgfr1 KO*. Nevertheless, the progressive elimination of binding of more and more signaling proteins to the receptor resulted in increasingly severe defects in vivo (Brewer et al., 2015). This suggests that in their system, Fgfr1 uses multiple signaling proteins additively to achieve full function in vivo. Additive use of different pathways has also been shown for Pdgfr-beta (Tallquist, French, & Soriano, 2003). Future studies are required to address these potential mechanisms for a better understanding of the complexities of Fgfr signaling in vivo in the oligodendrocyte lineage cells.

In addition to Fgfrs, Frs adapters are also known to bind and transmit signals from other tyrosine kinase receptors, including neurotrophin receptors, EGF receptors, RET, and ALK (Brewer et al., 2016; Degoutin, Vigny, & Gouzi, 2007; Huang et al., 2006; Kurokawa et al., 2001). Therefore, although our Fgfr2-Frs2/3 uncoupling experiment suggested that Frs2 adapters do not play a major role in transmitting Fgfr2-mediated signals for myelin growth, a formal possibility existed that Frs2/3 may have a function downstream of other receptors that are known to bind Frs2. Among these, the neurotrophin receptor TrkB was of special interest, since conditional ablation of TrkB in oligodendrocytes resulted in the formation of myelin sheaths thinner than normal, a phenotype similar to that observed in the *Fgfr2 cKO* mice (Xiao et al., 2010). However, since our analysis of mice with *complete* oligodendrocyte-specific ablation of Frs2/3 also showed only minor deficits in myelin gene expression and myelin thickness, it indicates that similar to Fgfr2, TrkB also does not fully rely on Frs2/3 to transduce its signals for myelin growth during the active period of myelination in the postnatal CNS.

Our previous in vivo studies have shown that in oligodendrocytes, Fgfr2 regulates myelin gene expression and myelin growth through the activation of ERK1/2, which in turn promotes mTORC1 activity in an Akt-independent manner (Furusho et al., 2017). Fgfrs are capable of activating ERK1/2 through multiple immediate downstream targets, including Frs2, Frs3, Gbr14, and Crk adapter proteins, as well as PLC gamma. Therefore, our data here showing only a modest decrease in p-ERK1/2 expression in oligodendrocyte cell bodies upon loss of Fgfr2-Frs2 binding, compared to an almost-complete loss in the *Fgfr2 cKO* mice, shown in our previous study (Furusho et al., 2012), suggest that it is likely that additive signaling by other proteins/adapters recruited by Fgfr2, along with Frs2, may be required within mature oligodendrocytes for the full activation of ERK1/2, leading to the optimal upregulation of myelin gene expression and myelin growth. It is not surprising that the modest downregulation of p-ERK1/2 in oligodendrocytes of the Fgfr2-Frs2-uncoupled mice was not sufficient to significantly downregulate myelin gene expression, since our previous studies (Ishii et al., 2012) have shown that presence of even one intact allele of either ERK1 or ERK2 was sufficient for oligodendrocytes to express almost-normal levels of myelin genes.

Our recent functional studies have shown that Fgfr2-mediated regulation of myelin gene expression and myelin growth during developmental myelination via ERK1/2 involves signaling through mTORC1 in an Akt-independent manner (Furusho et al., 2017; Ishii et al., 2019). Therefore, our findings here that the expression of p-mTOR and its downstream effector p-S6RP remained normal in mice lacking Frs2 function in spite of a partial reduction of ERK1/2 expression could also account for the lack of a more significant effect on myelin gene expression in these mutant mice.

In conclusion, our studies highlight the complexities of FGF signaling and reveal a previously unrecognized selectivity shown by Fgfrs in the use of Frs2 adapter proteins to carry out distinct functions (OPC specification vs myelin growth) during different stages of myelinogenesis. These studies are significant, as they provide basic insights about how cell surface tyrosine kinase receptors in vivo can potentially translate a common extracellular signal into distinct cellular responses during different stages of the oligodendrocyte developmental pathway, a mechanism that is likely to be adopted by cells of other lineages, as well.

ACKNOWLEDGMENTS

This work was supported by the NIH, Grant NS38878. We would like to thank Dr. V.P. Eswarakumar, Yale University, New Haven, for providing us the Fgfr2-delta *Frs2* mice, Dr. Jean Hebert (Albert Einstein College of Medicine, Bronx, NY) for Frs2 floxed/Frs3$^{-/-}$ mice, Dr. K-A Nave (Max Planck Institute of Experimental Medicine, Goettingen, Germany) for the *Cnp-Cre* mice, and Dr. D.M. Ornitz (Washington University School of Medicine, St. Louis, MI) for the *Fgfr1* and *Fgfr2* floxed mice.

Funding information

Foundation for the National Institutes of Health, Grant/Award Number: 5R37NS038878

REFERENCES

Bansal R, Kumar M, Murray K, Morrison RS, & Pfeiffer SE (1996). Regulation of FGF receptors in the oligodendrocyte lineage. Molecular and Cellular Neuroscience, 7, 263–275. 10.1006/mcne.1996.0020 [PubMed: 8793862]

Bansal R, Lakhina V, Remedios R, & Tole S. (2003). Expression of FGF receptors 1, 2, 3 in the embryonic and postnatal mouse brain compared with Pdgfralpha, Olig2 and Plp/dm20: Implications for oligodendrocyte development. Developmental Neuroscience, 25, 83–95. 10.1159/000072258 [PubMed: 12966207]

Beenken A, & Mohammadi M. (2009). The FGF family: Biology, pathophysiology and therapy. Natature Reviews Drug Discovery, 8(3), 235–253. 10.1038/nrd2792 [PubMed: 19247306]

Brewer JR, Mazot P, & Soriano P. (2016). Genetic insights into the mechanisms of Fgf signaling. Genes & Development, 30(7), 751–771. 10.1101/gad.277137.115 [PubMed: 27036966]

Brewer JR, Molotkov A, Mazot P, Hoch RV, & Soriano P. (2015). Fgfr1 regulates development through the combinatorial use of signaling proteins. Genes & Development, 29(17), 1863–1874. 10.1101/gad.264994.115 [PubMed: 26341559]

Bryant MR, Marta CB, Kim FS, & Bansal R. (2009). Phosphorylation and lipid raft association of fibroblast growth factor receptor-2 in oligodendrocytes. Glia, 57, 936–945. 10.1002/glia.20818

Degoutin J, Vigny M, & Gouzi JY (2007). ALK activation induces Shc and FRS2 recruitment: Signaling and phenotypic outcomes in PC12 cells differentiation. FEBS Letters, 581, 727–734. 10.1016/j.febslet.2007.01.039 [PubMed: 17274988]

Du Y, Lercher LD, Zhou R, & Dreyfus CF (2006). Mitogen-activated protein kinase pathway mediates effects of brain-derived neurotrophic factor on differentiation of basal forebrain oligodendrocytes. Journal of Neuroscience Research, 84, 1692–1702. 10.1002/jnr.21080 [PubMed: 17044032]

Eswarakumar VP, Ozcan F, Lew ED, Bae JH, Tomé F, Booth CJ, … Schlessinger J. (2006). Attenuation of signaling pathways stimulated by pathologically activated FGF-receptor 2 mutants prevents craniosynostosis. Proceedings of the National Academy of Sciences of the United States of America, 103(49), 18603–18608. 10.1073/pnas.0609157103 [PubMed: 17132737]

Fortin D, Rom E, Sun H, Yayon A, & Bansal R. (2005). Distinct fibroblast growth factor (FGF)/FGF receptor signaling pairs initiate diverse cellular responses in the oligodendrocyte lineage. Journal of Neuroscience, 25, 7470–7479. 10.1523/JNEUROSCI.2120-05.2005 [PubMed: 16093398]

Furusho M, Dupree JL, Nave KA, & Bansal R. (2012). Fibroblast growth factor receptor signaling in oligodendrocytes regulates myelin sheath thickness. Journal of Neuroscience, 32(19), 6631–6641. 10.1523/JNEUROSCI.6005-11.2012 [PubMed: 22573685]

Furusho M, Ishii A, & Bansal R. (2017). Signaling by FGF receptor 2, not FGF receptor 1, regulates myelin thickness through activation of ERK1/2-MAPK, which promotes mTORC1 activity in an Akt-independent manner. Journal of Neuroscience, 37(11), 2931–2946. 10.1523/JNEUROSCI.3316-16.2017 [PubMed: 28193689]

Furusho M, Kaga Y, Ishii A, Hébert JM, & Bansal R. (2011). Fibroblast growth factor signaling is required for the generation of oligodendrocyte progenitors from the embryonic forebrain. Journal of Neuroscience, 31(13), 5055–5066. 10.1523/JNEUROSCI.4800-10.2011 [PubMed: 21451043]

Fyffe-Maricich SL, Schott A, Karl M, Krasno J, & Miller RH (2013). Signaling through ERK1/2 controls myelin thickness during myelin repair in the adult central nervous system. Journal of Neuroscience, 33 (47), 18402–18408. 10.1523/JNEUROSCI.2381-13.2013 [PubMed: 24259565]

Gotoh N. (2008). Regulation of growth factor signaling by FRS2 family docking/scaffold adaptor proteins. Cancer Science, 99(7), 1319–1325. 10.1111/j.1349-7006.2008.00840.x [PubMed: 18452557]

Gravel M, Di Polo A, Valera PB, & Braun PE (1998). Four-kilobase sequence of the mouse CNP gene directs spatial and temporal expression of lacZ in transgenic mice. Journal of Neuroscience, 53, 393–404. 10.1002/(SICI)1097-4547(19980815)53:4<393::AID-JNR1>3.0.CO;2-1, PMID: 9710259

Huang L, Watanabe M, Chikamori M, Kido Y, Yamamoto T, Shibuya M, … Tsuchida N. (2006). Unique role of SNT-2/FRS2b/FRS3 docking/adaptor protein for negative regulation in EGF

receptor tyrosine kinase signaling pathways. Oncogene, 25, 6457–6466. 10.1038/sj.onc.1209656 [PubMed: 16702953]

Ishii A, Furusho M, & Bansal R. (2013). Sustained activation of ERK1/2 MAPK in oligodendrocytes and Schwann cells enhances myelin growth and stimulates oligodendrocyte progenitor expansion. Journal of Neuroscience, 33(1), 175–186. 10.1523/JNEUROSCI.4403-12.2013 [PubMed: 23283332]

Ishii A, Furusho M, Dupree JL, & Bansal R. (2014). Role of ERK1/2 MAPK signaling in the maintenance of myelin and axonal integrity in the adult CNS. Journal of Neuroscience, 34(48), 16031–16045. 10.1523/JNEUROSCI.3360-14.2014 [PubMed: 25429144]

Ishii A, Furusho M, Dupree JL, & Bansal R. (2016). Strength of ERK1/2 MAPK activation determines its effect on myelin and axonal integrity in the adult CNS. Journal of Neuroscience, 36(24), 6471–6487. 10.1523/JNEUROSCI.0299-16.2016 [PubMed: 27307235]

Ishii A, Furusho M, Macklin W, & Bansal R. (2019). Independent and cooperative roles of the Mek/ERK1/2-MAPK and PI3K/Akt/mTOR pathways during developmental myelination and in adulthood. Glia, 67(7), 1277–1295. 10.1002/glia.23602 [PubMed: 30761608]

Ishii A, Fyffe-Maricich SL, Furusho M, Miller RH, & Bansal R. (2012). ERK1/ERK2 MAPK signaling is required to increase myelin thickness independent of oligodendrocyte differentiation and initiation of myelination. Journal of Neuroscience, 32(26), 8855–8864. 10.1523/JNEUROSCI.0137-12.2012 [PubMed: 22745486]

Jeffries MA, Urbanek K, Torres L, Wendell SG, Rubio ME, & Fyffe-Maricich SL (2016). ERK1/2 activation in preexisting oligodendrocytes of adult mice drives new myelin synthesis and enhanced CNS function. Journal of Neuroscience, 36(35), 9186–9200. 10.1523/JNEUROSCI.1444-16.2016 [PubMed: 27581459]

Kaga Y, Shoemaker WJ, Furusho M, Bryant M, Rosenbluth J, Pfeiffer SE, … Bansal R. (2006). Mice with conditional inactivation of fibroblast growth factor receptor-2 signaling in oligodendrocytes have normal myelin but display dramatic hyperactivity when combined with Cnp1 inactivation. Journal of Neuroscience, 26(47), 12339–12350. 10.1523/JNEUROSCI.3573-06.2006 [PubMed: 17122059]

Kahn MA, Kumar S, Liebl D, Chang R, Parada LF, & De Vellis J. (1999). Mice lacking NT-3, and its receptor TrkC, exhibit profound deficiencies in CNS glial cells. Glia, 26, 153–165. PMID: 10384880 [PubMed: 10384880]

Kurokawa K, Iwashita T, Murakami H, Hayashi H, Kawai K, & Takahashi M. (2001). Identification of SNT/FRS2 docking site on RET receptor tyrosine kinase and its role for signal transduction. Oncogene, 20, 1929–1938. 10.1038/sj.onc.1204290 [PubMed: 11360177]

Lappe-Siefke C, Goebbels S, Gravel M, Nicksch E, Lee J, Braun PE, … Nave KA (2003). Disruption of Cnp1 uncouples oligodendroglial functions in axonal support and myelination. Nature Genetics, 33(3), 366–374. 10.1038/ng1095 [PubMed: 12590258]

Mason I. (2007). Initiation to end point: The multiple roles of fibroblast growth factors in neural development. Nature Reviews Neuroscience, 8, 583–596. 10.1038/nrn2189 [PubMed: 17637802]

Nandi S, Gutin G, Blackwood CA, Kamatkar NG, Lee KW, Fishell G, … Hébert JM (2017). FGF-dependent, context-driven role for FRS adapters in the early telencephalon. Journal of Neuroscience, 37(23), 5690–5698. 10.1523/JNEUROSCI.2931-16.2017 [PubMed: 28483978]

Ornitz D, & Itoh N. (2015). The fibroblast growth factor signaling pathway. Wiley Interdisciplinary Reviews: Developmental Biology, 4(3), 215–266. 10.1002/wdev.176 [PubMed: 25772309]

Sims-Lucas S, Cusack B, Eswarakumar VP, Zhang J, Wang F, & Bates CM (2011). Independent roles of Fgfr2 and Frs2alpha in ureteric epithelium. Development, 138(7), 1275–1280. 10.1242/dev.062158 [PubMed: 21350013]

Tallquist MD, French WJ, & Soriano P. (2003). Additive effects of PDGF receptor β signaling pathways in vascular smooth muscle cell development. PLoS Biology, 1(2), E52. 10.1371/journal.pbio.0000052 [PubMed: 14624252]

Tognatta R, Sun W, Goebbels S, Nave KA, Nishiyama A, Schoch S, Dimou L, & Dietrich D 2017. Transient cnp expression by early progenitors causes Cre-Lox-based reporter lines to map profoundly different fates. Glia 65, 342–359. 10.1002/glia.23095, PMID: 27807896 [PubMed: 27807896]

Turner N, & Grose R. (2010). Fibroblast growth factor signalling: From development to cancer. Nature Reviews Cancer, 10, 116–129. 10.1038/nrc2780 [PubMed: 20094046]

Xiao J, Wong AW, Willingham MM, van den Buuse M, Kilpatrick TJ, & Murray SS (2010). Brain-derived neurotrophic factor promotes central nervous system myelination via a direct effect upon oligodendrocytes. Neurosignals, 18(3), 186–202. 10.1159/000323170 [PubMed: 21242670]

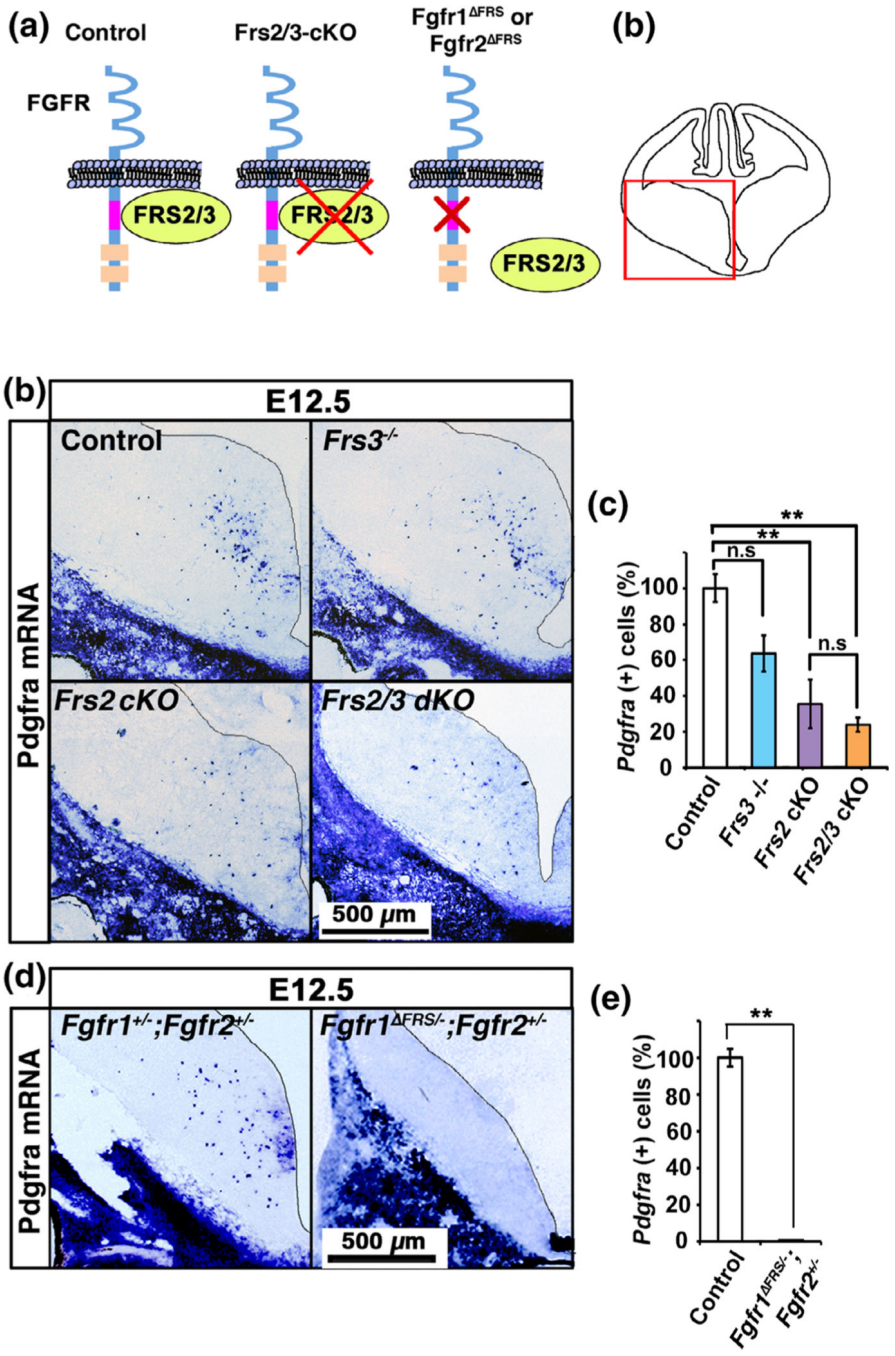

FIGURE 1.

Genetically disrupting binding of Frs2 to Fgfr1 or its complete ablation in embryonic forebrain cells leads to severe deficits in the specification of OPCs at E12.5. Diagram showing (a) the mutants used in the study and the mouse embryonic forebrain region (marked by red box) shown in (b) and (d). (b, c)Coronal sections of E12.5 forebrains from control, *Frs3*$^{-/-}$, *Frs2 cKO*, and *Frs2/3 dKO* mice, analyzed by in situ hybridization for the expression of OPC marker Pdgfra mRNA, show that compared to control, there is a significant reduction in the numbers of Pdgfra+ cells in the *Frs2 cKO* and *Frs2/3*

dKO but not in the *Frs3*$^{-/-}$ embryos. (d) E12.5 forebrains from *Fgfr1*$^{+/-}$;*Fgfr2*$^{+/-}$ and *Fgfr1*$^{\Delta Frs/-}$;*Fgfr2*$^{+/-}$ mice, analyzed for the expression of Pdgfra mRNA, show an almost complete loss of Pdgfra+ OPCs in the *Fgfr1*$^{\Delta Frs/-}$;*Fgfr2*$^{+/-}$ compared to *Fgfr1*$^{+/-}$;*Fgfr2*$^{+/-}$ embryos. This is confirmed by the quantification of the total numbers of Pdgfra mRNA positive cells in the whole caudal forebrains from control and mutant mice. Three matched sections each from two to four embryos of each genotype were analyzed and the data is expressed as percentage of control. Scale bars, as indicated. Error bars indicate *SEM*. $^{**}p < .01$; ns, not significant [Color figure can be viewed at wileyonlinelibrary.com]]

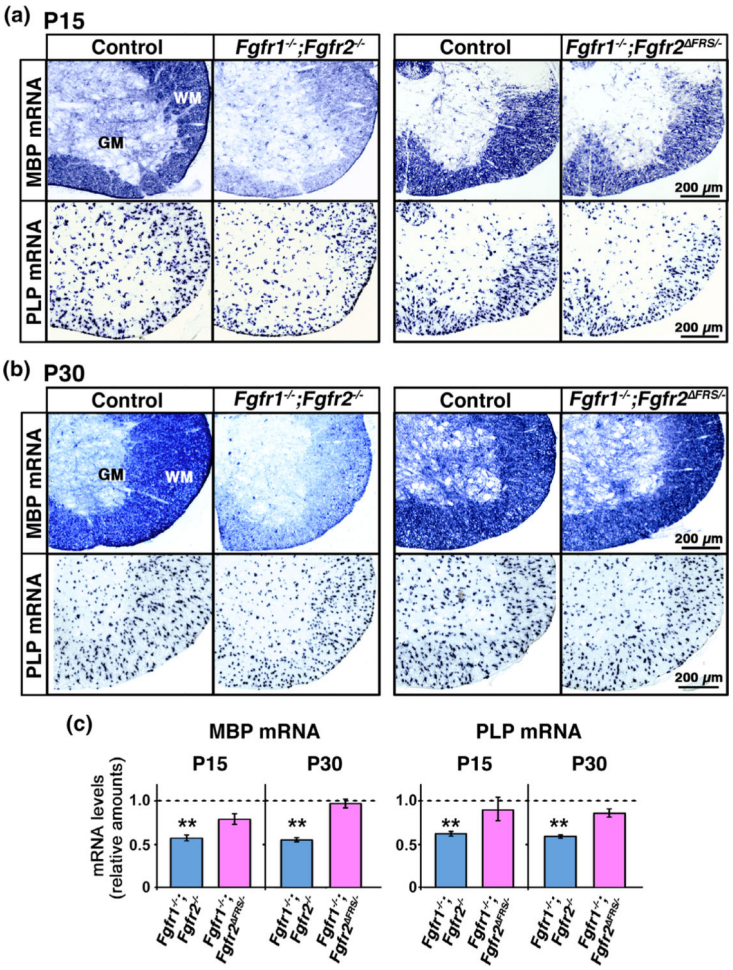

FIGURE 2.

Fgfr1/2 mutants with disruption of Frs2/3 binding to Fgfr2 in oligodendrocytes of the postnatal spinal cord fail to recapitulate the severe deficits in myelin gene expression observed in the conditional Fgfr1/2 knock-out mice. Transverse section of cervical spinal cord at P15 (a) and P30 (b) analyzed by in situ hybridization for MBP and PLP mRNA from control, *Fgfr1*$^{-/-}$;*Fgfr2*$^{-/-}$, and *Fgfr1*$^{-/-}$;*Fgfr2*$^{\Delta Frs/-}$ mice shows a clear reduction in their signal intensity in the *Fgfr1*$^{-/-}$;*Fgfr2*$^{-/-}$ mice compared to controls. At P15, *Fgfr1*$^{-/-}$;*Fgfr2*$^{\Delta Frs/-}$ mice also show a slight reduction in MBP and PLP mRNA signal intensity compared to control, but the reduction is not as much as in *Fgfr1*$^{-/-}$;*Fgfr2*$^{-/-}$ mice. (c) Quantification of mRNA levels by qRT-PCR in P15 and P30 spinal cords shows a statistically significant reduction in the expression of MBP and PLP mRNA levels in the *Fgfr1*$^{-/-}$;*Fgfr2*$^{-/-}$ but not in the *Fgfr1*$^{-/-}$;*Fgfr2*$^{\Delta Frs/-}$ mice compared to controls. The control value, set at 1.0, is shown as a dotted line. Three to five mice of each group were analyzed. Scale bar, as indicated. Error bars indicate *SEM*. $^{**}p < .01$. WM, white matter; GM, grey matter [Color figure can be viewed at wileyonlinelibrary.com]]

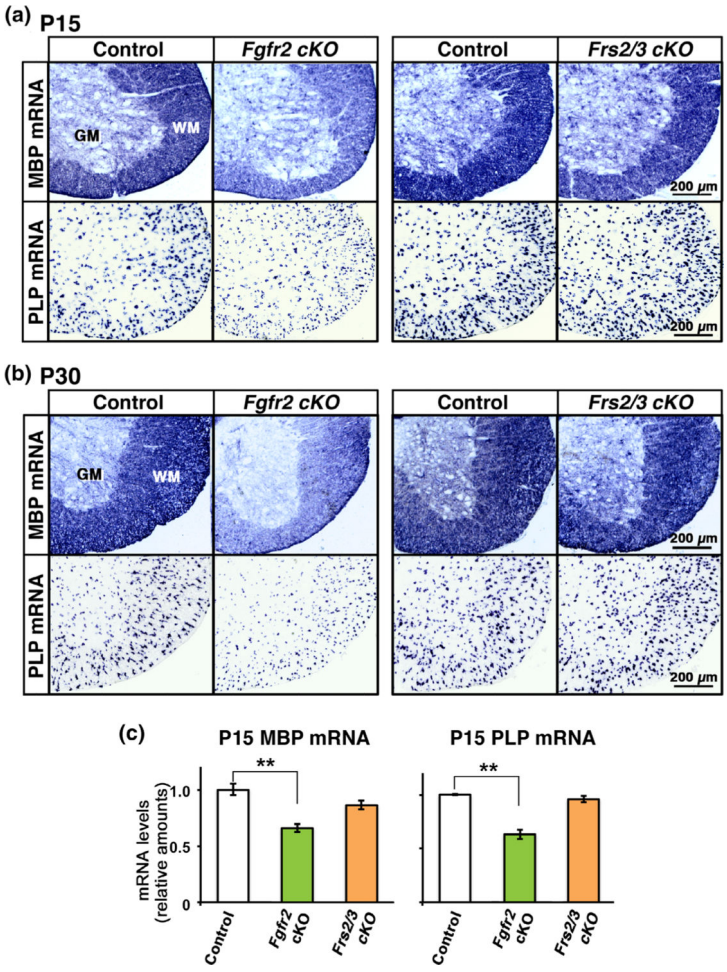

FIGURE 3.

Complete ablation of Frs2/3 in oligodendrocytes of the postnatal spinal cord fails to recapitulate the deficits in myelin gene expression observed in the conditional Fgfr2 knock-out mice. Transverse section of cervical spinal cord at P15 (a) and P30 (b) analyzed by in situ hybridization for MBP and PLP mRNA from control, *Fgfr2 cKO*, and *Frs2/3 cKO* mice shows reduced signal intensity in *Fgfr2 cKO* compared to controls at both time points. Although MBP mRNA signal in the *Frs2/3 cKO* appears to be slightly reduced at P15 compared to control, it is comparable to control at P30. (c) Quantification of mRNA levels by qRT-PCR in P15 spinal cords shows a significant reduction in the expression of MBP and PLP mRNA levels in the *Fgfr2 cKO* but not in the *Frs2/3 cKO* compared to control mice. Three to six mice of each group were analyzed. Scale bar, as indicated. Error bars indicate *SEM*. $^{**}p < .01$. WM, white matter; GM, grey matter [Color figure can be viewed at wileyonlinelibrary.com]

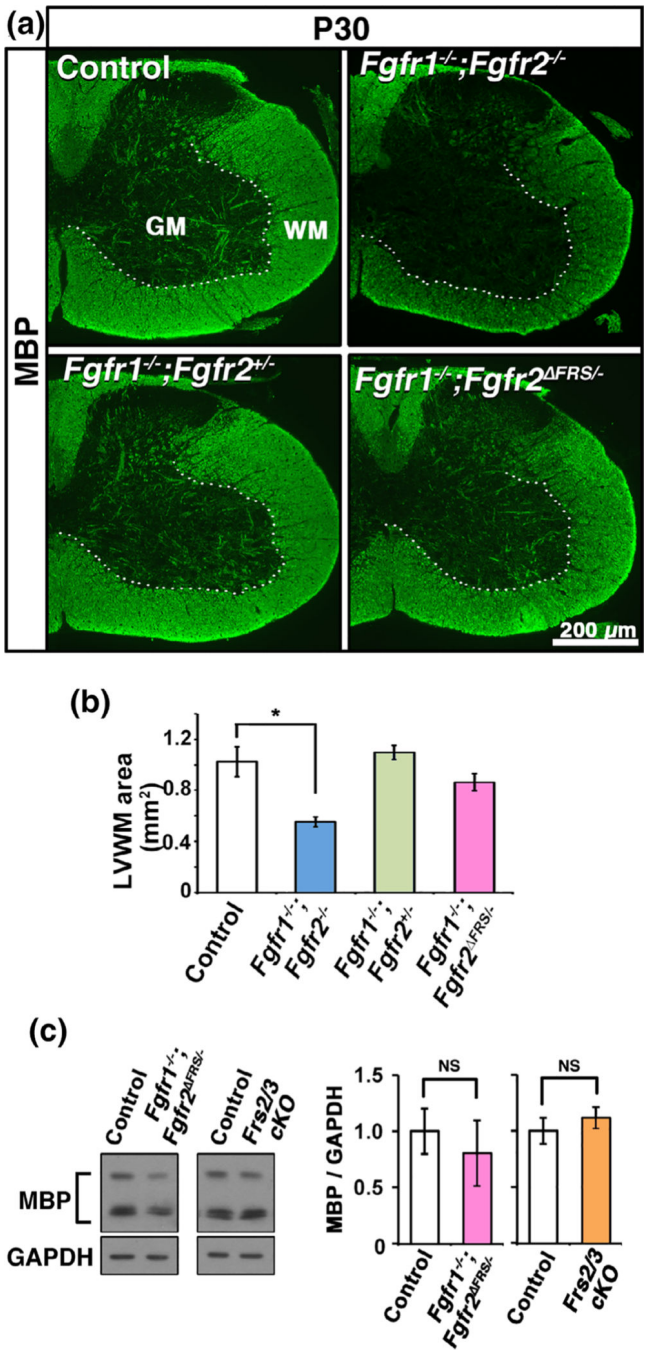

FIGURE 4.

Fgfr1/2 mutants with disruption of Frs2/3 binding to Fgfr2 in oligodendrocytes fail to show a downregulation of myelin basic protein expression or a reduction in white matter area as observed in the conditional Fgfr1/2 knock-out mice (a) Cervical spinal cord sections from P30 control, *Fgfr1*$^{-/-}$;*Fgfr2*$^{-/-}$, *Fgfr1*$^{-/-}$;*Fgfr2*$^{+/-}$, and *Fgfr1*$^{-/-}$;*Fgfr2*$^{\Delta Frs/-}$ mice immunolabeled for MBP show that the intensity of MBP signal and the size of the white matter area are reduced in *Fgfr1*$^{-/-}$;*Fgfr2*$^{-/-}$ mice compared to control or *Fgfr1*$^{-/-}$;*Fgfr2*$^{+/-}$, but this reduction is not seen in the *Fgfr1*$^{-/-}$;*Fgfr2*$^{\Delta Frs/-}$ mice. (a) Quantification of

the total area of the MBP+ lateral-ventral white matter (LVWM) also shows a decrease in the size of the white matter in the *Fgfr1*$^{-/-}$;*Fgfr2*$^{-/-}$ compared to control or *Fgfr1*$^{-/-}$;*Fgfr2*$^{+/-}$ but not in the *Fgfr1*$^{-/-}$;*Fgfr2*$^{\Delta Frs/-}$ mice. (c) Immunoblotting of equal amounts of total proteins from homogenates of whole cervical spinal cord and quantification of the signal intensities of MBP protein isoforms (bracket) show no significant reduction in their levels at P15 in the *Fgfr1*$^{-/-}$;*Fgfr2*$^{\Delta Frs/-}$ or the *Frs2/3 cKO* mice compared to their respective controls. GAPDH is used as a loading control. Error bars represent *SEM*. $N = 3–8$, $*p < .05$. NS, not significant. Scale bar, as indicated. WM, white matter, GM, grey matter [Color figure can be viewed at wileyonlinelibrary.com]]

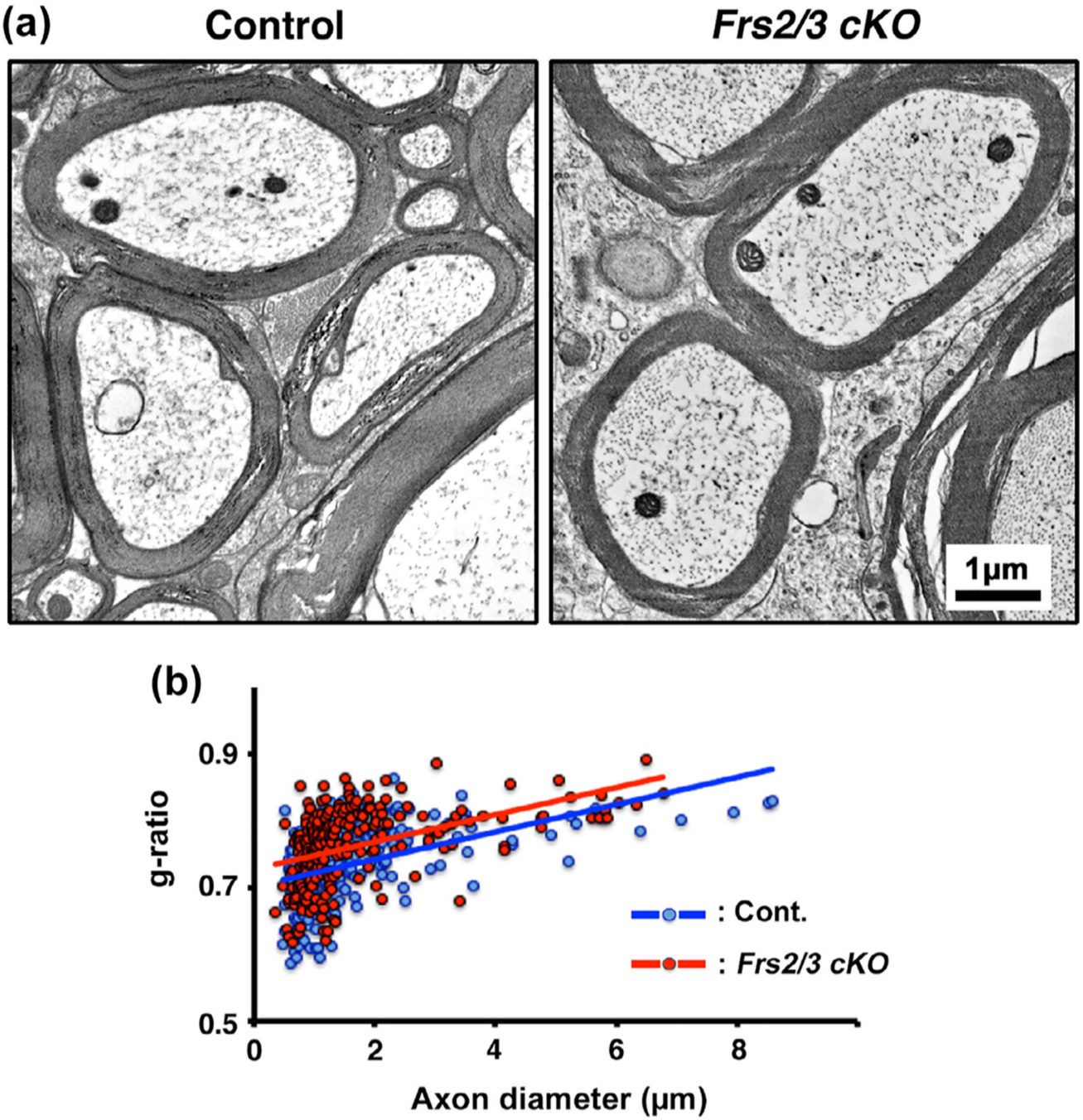

FIGURE 5.

Complete ablation of Frs2/3 in oligodendrocytes did not lead to a significant reduction in myelin thickness in the spinal cords of adult mice. (a) EM images taken from matched regions of the ventral cervical spinal cord white matter at 5 months of age show that the thickness of myelin in the *Frs2/3 cKO* mice appears to be similar to that in their littermate controls. (b) Quantification of myelin thickness by g-ratio analysis, presented as scatter plots relative to axon diameters shows a trend towards thinner myelin sheaths in the mutants, indicated by slightly higher g-ratios in the *Frs2/3 cKO* mice (red dots; average g-ratios =

0.762 +/−0.004) compared to its littermate control (blue dots; average g-ratios = 0.736 +/− 0.004, $p = 9.35 \times 10^{-7}$). Approximately 200–400 axons from two mice of each genotype were analyzed. Representative images of spinal cords taken from similar regions of lateral-ventral white matter from the control and mutant mice are shown. Scale bar, as indicated [Color figure can be viewed at wileyonlinelibrary.com]]

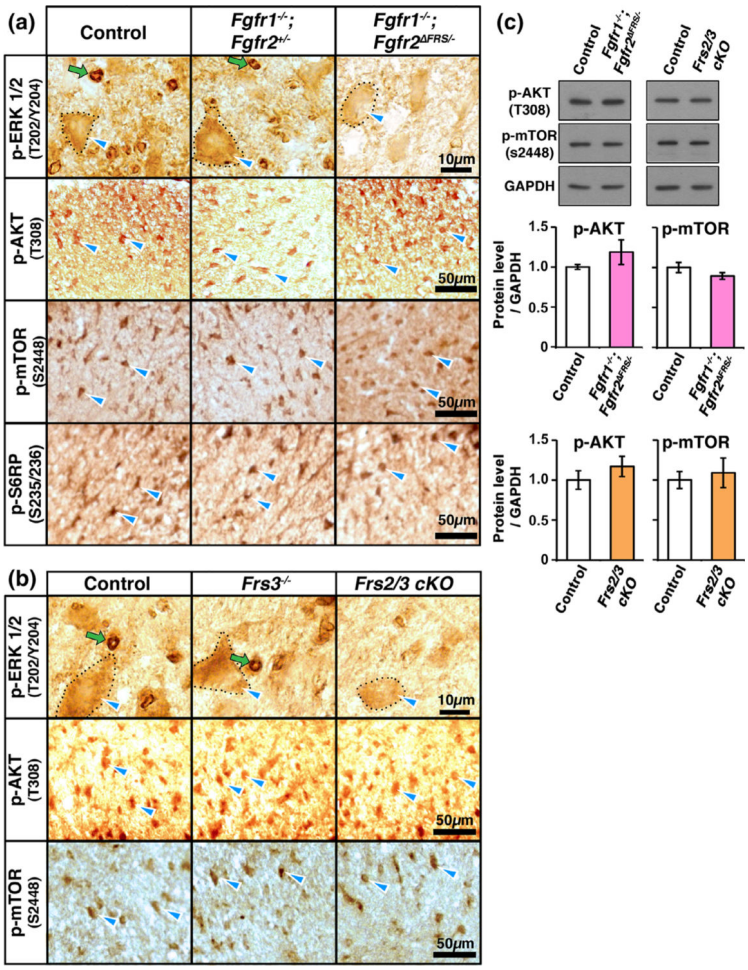

FIGURE 6.

p-ERK1/2 expression is partly reduced but p-Akt, p-mTOR and p-S6RP remain unchanged in oligodendrocytes of mice with disruption of Frs2/3 binding to Fgfr2 or with complete ablation of Frs2/3 in oligodendrocytes. Cervical spinal cord sections at P15, immunolabeled for p-ERK1/2, show oligodendrocyte-like cellular staining (outlined in dotted line, blue arrowhead) and "ring-like" paranodal staining (green arrows) in the white matter of control, *Fgfr1*$^{-/-}$*;Fgfr2*$^{+/-}$ (a), and *Frs3*$^{-/-}$ (b) mice. Compared to this pattern in the controls, the oligodendrocyte-like cellular staining of p-ERK1/2 is slightly decreased, but the "ring-like" staining is significantly reduced in the *Fgfr1−/−; Fgfr2ΔFrs/−* (a) and *Frs2/3 cKO* (b) mice (numbers of "rings" counted in the white matter of control = 440.09+/− 32.9, and *Frs2/3 cKO* = 78.82 +/− 9.2mm^2). The intensity of the cellular signal for pAkt^{308}, p-mTOR^{S2448}, and p-S6RP$^{S235/236}$ remains comparable to controls for all genotypes. (c) Immunoblotting of equal amounts of total proteins from homogenates of cervical spinal cord and quantification of the band intensities show that p-AKT and p-mTOR expression levels are not significantly reduced at P15 in the *Fgfr1*$^{-/-}$*;Fgfr2*$^{\Delta Frs/-}$ or *Frs2/3 cKO* mice compared to their respective controls. GAPDH is used as a loading control. Error bars represent *SEM*. *N* = 3–7 for each genotype. Scale bars as indicated. Representative images

taken from similar regions of lateral-ventral white matter are shown [Color figure can be viewed at wileyonlinelibrary.com]]